Journal of the European Ceramic Society 21 (2001) 1945–1949
www.elsevier.com/locate/jeurceramsoc

Sintering of MnZn-ferrite powders prepared by hydrothermal reactions between oxides

Darko Makovec[a,*], Miha Drofenik[a], Andrej Žnidaršič[b]

[a]*Department of Ceramics, Jožef Stefan Institute, Ljubljana, Slovenia*
[b]*ISKRA Feriti, Ljubljana, Slovenia*

Received 4 September 2000; received in revised form 19 October 2000; accepted 25 October 2000

Abstract

The sintering of ferrite powders prepared by a hydrothermal treatment of starting oxides was studied in comparison with conventional pre-sintered powders. Two hydrothermal powders were prepared, one with a similar degree of conversion into spinel products as the pre-sintered powder but with a larger specific surface, and the other with a lower specific surface area and a high degree of conversion into $MnZnFe_2O_4$. In the first powder, non-homogeneity caused primarily by the agglomeration of the Mn-rich particles (Mn_3O_4 and $ZnMn_2O_4$) resulted in the formation of Kirkendall porosity, which significantly influenced the densification process. © 2001 Elsevier Science Ltd. All rights reserved.

Keywords: Ferrites; Porosity; Powders: chemical preparation; Sintering; Soft magnets

1. Introduction

The large-scale production of MnZn-ferrite ceramic materials is based on ceramic technology involving pre-sintering of a homogenized mixture of the appropriate starting oxides at temperatures around 900°C in air. This pre-sintered material is subsequently milled to produce the ferrite powder. The pre-sintering step has the following effects on the ferrite powder:[1] (i) oxides are partially transformed into various spinel phases, (ii) the variations in reactivity of the individual starting oxides are reduced and (iii) the starting mixture is homogenized. This last effect is believed to have the largest influence on the properties of the final sintered ferrites.[1]

An alternative method involves the preparation of ferrite powders by the hydrothermal treatment of starting oxides.[2] During hydrothermal treatment, chemical reactions between oxides occur in an autoclave at elevated temperatures around 300°C under a high pressure, normally under equilibrium water pressure. As a result of the hydrothermal treatment, multiphase powders are obtained, composed of some residual reactants (Fe_2O_3, Mn_3O_4) and spinel products, e.g. ferrite $Zn(Mn)Fe_2O_4$ and manganate $ZnMn_2^{3+}O_4$. The nature of the spinel products formed as well as the degree of conversion into the products is a function mainly of the oxidation state of the manganese present during treatment. To obtain a high degree of conversion to $MnZnFe_2O_4$, the starting oxide mixture containing MnO has to be hydrothermally treated under an inert atmosphere.[3]

Hydrothermally derived powders are much finer than conventionally prepared powders using pre-sintering. Their high reactivity demands special attention during sintering. The aim of the present work was to study the sintering of the hydrothermally derived powders in comparison to the conventional pre-sintered powder.

2. Experimental

Two different ferrite powders with a composition corresponding to the formula $Mn_{0.50}Zn_{0.42}Fe_{2.07}O_4$ were prepared using a hydrothermal treatment of the intimate mixture of starting oxides: Fe_2O_3 (CSR 800, Chemirite LTD., specific surface area 6.0 m^2/g), ZnO (Zinkweiss Pharma A, 3.9 m^2/g) and Mn_3O_4 (Brownox-X, Tosoh Corp., 13.5 m^2/g) or MnO (Johnson Matthey, 0.6 m^2/g) for 2 h at 300°C under an equilibrium water pressure. The powder A was prepared using Mn_3O_4 as a source of manganese and the hydrothermal reaction was

---

[*] Corresponding author. Tel.: +386-1477-4579; fax: +386-1426-3126.
E-mail address: darko.makovec@ijs.si (D. Makovec).

PII: S0955-2219(01)00148-0

conducted in air, while for powder B, MnO was used for hydrothermal reaction under an inert atmosphere. Details of the hydrothermal method used are explained in Ref. 3. After the hydrothermal treatment, the powders were milled in a steel ball mill for additional homogenization and deagglomeration.

For the comparison, powder C was prepared using classic ceramic technology by pre-sintering of the starting oxide mixture with Mn_3O_4 for 1 h at 900°C in air and subsequent milling in a steel planetary ball mill for 4 h in an aqueous environment.

The powders were analyzed using quantitative X-ray powder diffractometry (XRPD),[3] thermal analysis (DTA/TGA), scanning (SEM) and transmission (TEM) electron microscopy and other methods.

To study the sintering process, the powders were granulated with 2 wt.% PVA and 0.5 wt.% PEG and pressed into tablets with a green density of 3.00 g/cm^3. Shrinkage of the samples during sintering was studied using a dilatometer (Type 802, Bähr Gerätebau GmbH,) at a constant heating rate of 5°C/min in air, or in N_2 containing less than 500 ppm O_2. The reactions occurring during sintering were studied using high-temperature diffractometry (HT-XRPD), SEM and DTA/TGA.

3. Results and discussion

3.1. *Analysis of the powders*

The powder A had the largest specific surface area (7.2 m^2/g) and the lowest degree of conversion into the spinel products. Phase-composition analysis using a combination of XRPD and TEM/EDS showed that powder A was composed of the remaining reactants Fe_2O_3 (~52 wt.%) and Mn_3O_4 (~6 wt.%), and of two spinel products, $ZnFe_2O_4$ and $ZnMn_2^{3+}O_4$. TGA analysis (Fig. 1) suggested that the manganese was present preferentially in the oxidation state 3+, since Mn_3O_4 was oxidized during the hydrothermal treatment in air. The particles of individual phases present in powder A had different shapes and sizes; the oblong particles of Fe_2O_3 and the octahedrally shaped crystallites of $ZnFe_2O_4$ were much larger (~ 0.3 μm in size) than the rounded Mn-rich particles of Mn_3O_4 and $ZnMn_2O_4$ (less than 0.1 μm in size). The small Mn-rich particles have a strong tendency to agglomerate [Fig. 2 (a)].

Powder B had a lower surface area (4.0 m^2/g) than powder A, but a much higher degree of conversion into the spinel products. In addition to Fe_2O_3 (~13 wt.%), it was composed mainly of (Mn^{2+}, Zn)Fe_2O_4 spinel and was much more homogeneous than powder A. The manganese in powder B was present preferentially in the oxidation state 2+. This can be demonstrated by TGA showing mass changes corresponding to the oxidation of MnO to Mn_2O_3 during heating in air (Fig. 1).

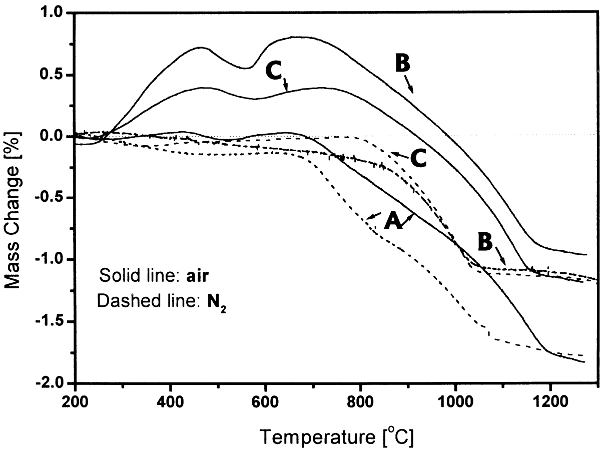

Fig. 1. Thermogravimetric measurements on samples heated in air and in N_2.

The conventional powder C had a surface area similar to powder B (4.6 m^2/g) and a degree of conversion similar to that of powder A (it contained ~52% of the remaining Fe_2O_3).

3.2. *Sintering*

During the heating of multiphase mixtures, the shrinking of the samples is often influenced by chemical reactions (reaction sintering). Fig. 3 shows changes in the relative intensity of the Fe_2O_3 (104) XRD peak with the temperature for the samples heated in air or in N_2. It can be seen that Fe_2O_3 is consumed by the (Mn^{2+}, Zn)Fe_2O_4-formation reaction at a higher rate when sintered in N_2 than in air. In N_2, the formation of (Mn^{2+}, Zn)Fe_2O_4 in all the samples was already completed after heating to 900°C, while in air, Fe_2O_3 grains were observed by SEM/EDS in sample A even after heating it to 1150°C. During heating in air at temperatures below ~ 700°C, the manganese present in the starting powder in the oxidation state 2+ is oxidized (Fig. 1) and consequently the $MnZnFe_2O_4$ present in the powder decomposes (intensity of Fe_2O_3 peaks increase with temperature for sample B, Fig. 3). During heating in N_2, the Mn^{2+} is preserved and consequently the ferrite-formation reaction is completed at a much lower temperature than in air.

Figs. 4 and 5 show the shrinkage curves and the corresponding shrinkage-rate spectra for the samples sintered in air and in N_2, respectively. During heating in air, a small step-like shrinkage at ~600°C is visible. This step-like shrinkage, which is largest for sample B, while hardly visible for sample A, is related to the oxidation reaction of Mn^{2+} (Ref. 4). In air, sample A starts to shrink at a lower temperature (~660°C) than sample B (~ 800°C). This is consistent with the fact that powder A exhibits the largest specific surface area. Moreover, the onset of shrinkage in sample B may be delayed due to oxi-

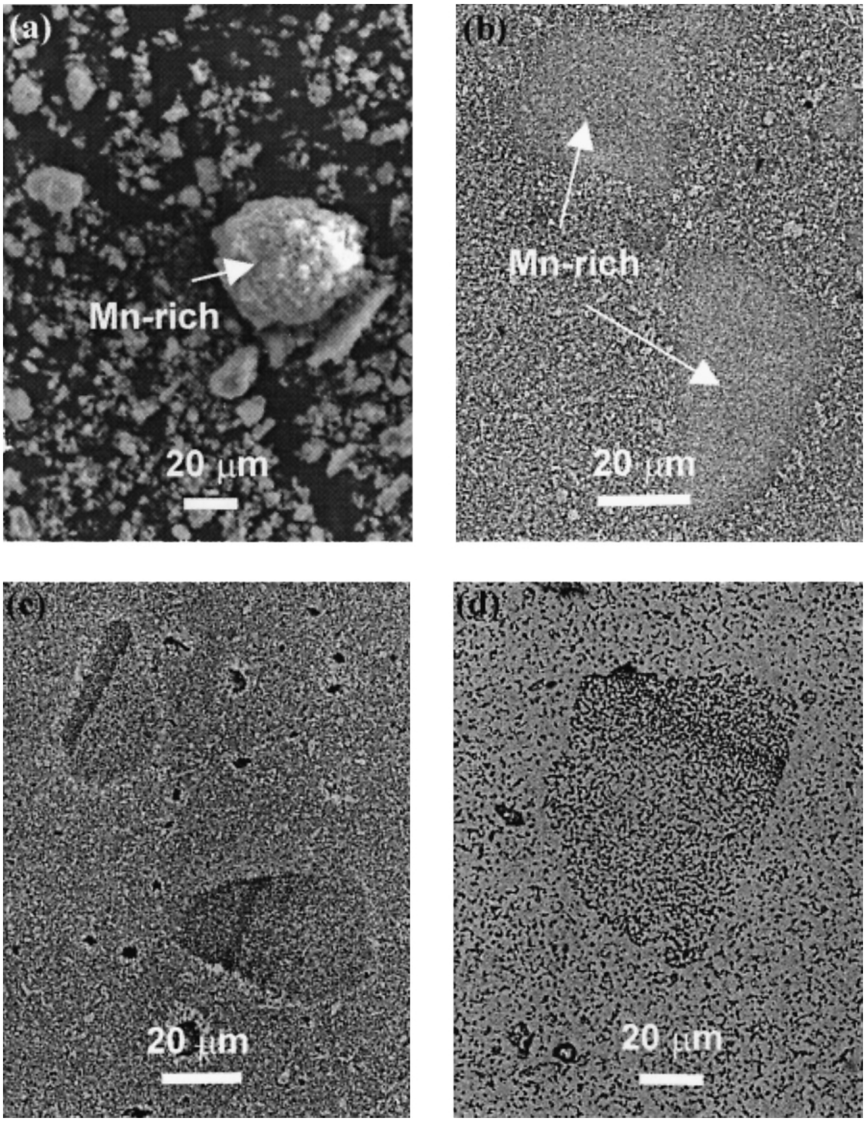

Fig. 2. SEM micrographs of powder A (a) and samples A, heated in air to 600°C (b), 900°C (c) and 1150°C (d) illustrating the formation of Kirkendall porosity.

dation reactions. During sintering in N_2, all three samples start to shrink at nearly the same temperature (~ 600°C), lower than during sintering in air.

Due to heterogeneity of the powders and the consequent chemical reactions accompanying the densification, the shrinkage-rate spectra exhibits two shrinkage-rate maxima [Figs. 4(b) and 5(b)]. The first maximum, at a lower temperature, is especially large for powder A, which has the largest surface area, the lowest degree of conversion into spinel products and is very non-homogeneous. The major influence on the non-homogeneity of this powder is the agglomeration of the Mn-rich particles in an aqueous environment. Due to counter-diffusion of the ions with different diffusivities, the ferrite-formation reactions are accompanied by the formation of large Kirkendall pores.[5] These large pores are visible in the microstructures of samples A, cooled from

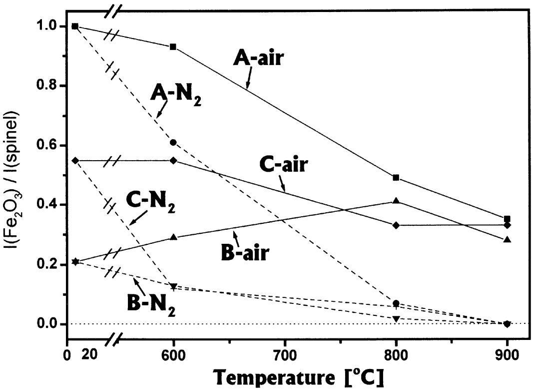

Fig. 3. Change in the intensity of the Fe_2O_3 (104) peak relative to the intensity of the spinel (311) peak with temperature illustrates the consumption of Fe_2O_3 for the ferrite-formation reaction or an increase in its concentration due to decomposition of $MnZnFe_2O_4$. High temperature-diffractometry was performed during heating in air or in N_2.

1000°C under equilibrium conditions [Figs. 4(a) and 5(a)].

Fig. 2 illustrates the formation of the Kirkendall pores. Mn from the large Mn-rich agglomerates present in powder A [Fig. 2(a) and (b)] diffuse into the surrounding matrix, leaving the Kirkendall pores behind [Fig. 2(c) and (d)]. At porous regions of the sample, much higher concentrations of Mn were detected by EDS, than in the surrounding matrix. The formation of pores may be additionally influenced by the oxygen release related to manganese reduction during its incorporation into the ferrite. Due to formation of Kirkendall pores related to the ferrite-formation reactions, the shrinkage rate is decreased, resulting in the first, low-temperature maximum in the shrinkage-rate spectra. In samples B and especially in the conventional samples C, where better homogeneity is expected than in sample A, this low-temperature maximum in the shrinkage-rate spectra are difficult to resolve, while large Kirkendall pores were very seldom observed. In the conventional sample C these effects are not pronounced in spite of the low conversion rate of the starting oxide mixture into the spinel products after the pre-sintering step in air, confirming the advantageous effect of the pre-sintering on the homogeneity of the ferrite powder.[1] The first low-temperature maximum appeared at lower temperatures during sintering in N_2 than in air, in agreement with the fact that in N_2 the ferrite-formation reactions occur at lower temperatures.

The maximum shrinkage rate, i.e. the second, high-temperature maximum in the shrinkage-rate spectra, could be related to sintering of the already-formed $MnZnFe_2O_4$. It was observed at temperatures around 1150°C in air and at higher temperatures (above 1200°C) in N_2. The final

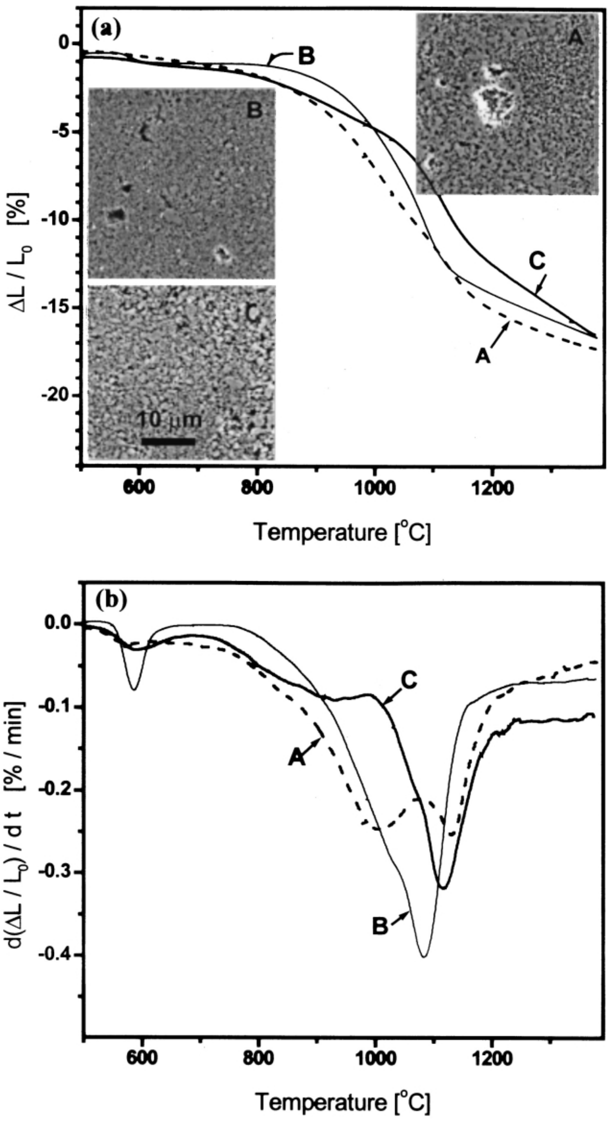

Fig. 4. Shrinkage curves (a) and corresponding shrinkage-rate spectra (b) for samples sintered in air. In (a) SEM micrographs of samples cooled under equilibrium conditions from 1000°C are inserted.

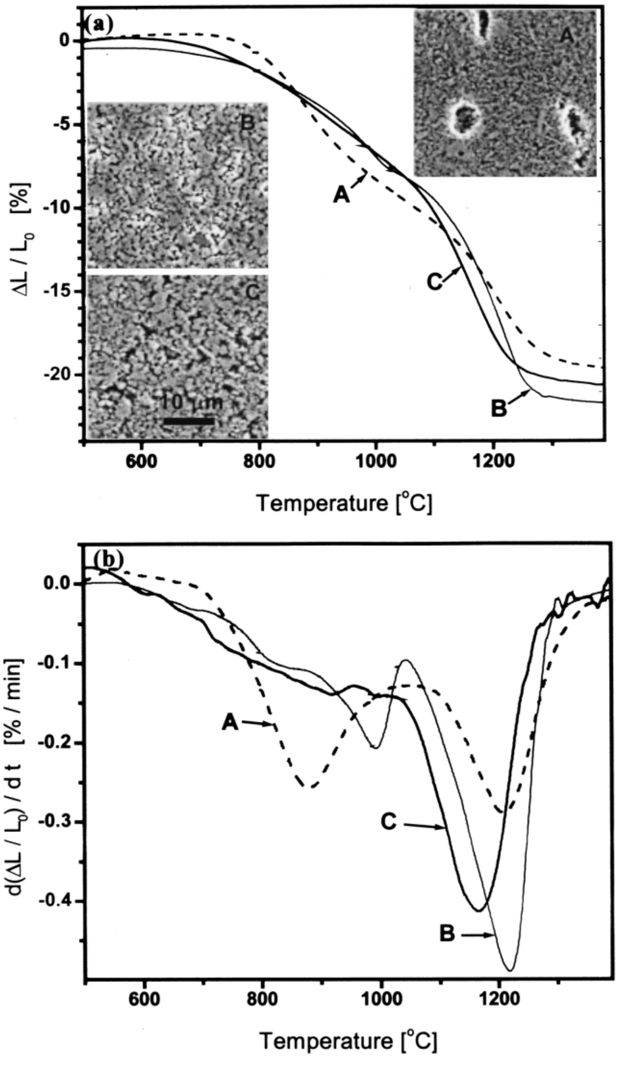

Fig. 5. Shrinkage curves (a) and corresponding shrinkage-rate spectra (b) for samples sintered in N_2. In (a) SEM micrographs of samples cooled from 1000°C are inserted.

shrinkage, as well as the maximum shrinking rate, was higher in N_2 than in air for all the samples. This can be explained by the increase in oxygen lattice diffusion during sintering under a low oxygen partial pressure.[6]

In the present investigation, relatively large differences in the sintering behavior have been observed between the hydrothermally prepared ferrite powders and the conventional pre-sintered powder. The hydrothermal powder A had the largest specific surface area and was the most reactive, however, the agglomeration of the Mn-rich particles during hydrothermal treatment negated the benefit of a large specific surface area.

4. Conclusions

This study of sintering has shown that ferrite powders prepared by the hydrothermal treatment of commercial raw oxides can be successfully used for the preparation of MnZn ferrites with improved properties when a sufficient homogeneity of the powder is achieved. To achieve this homogeneity, the agglomeration of individual phases (Mn-rich particles) in the aqueous environment of the hydrothermal treatment has to be prevented.

Acknowledgements

The authors would like to thank the Ministry of Science and Technology, Republic of Slovenia, for financial support.

References

1. Toolenaar, F. J. C. M., Effects of presintering on densification phenomena of ferrites. *Sol. State Ion.*, 1985, **16**, 267–274.
2. Lucke, R., Schlegel, E. and Strienitz, R., Hydrothermal preparation of manganese zinc ferrites. *Journal de Physique*, 1997, **III**, C1-63–C1-64.
3. Makovec, D., Žnidaršiè, A. and Drofenik, M., Hydrothermal synthesis of manganese zinc ferrite powders from oxides. *J. Am. Ceram. Soc.*, 1999, **82**(5), 113–120.
4. Perriat, P., Gillot, B. and Aymes, D., Oxidation and reduction reactions in spinel oxides: influence upon some physical properties. *Journal de Physique*, 1997, **III**, C1-43–C1-46.
5. Evano, P. Y. and Paulus, M. P., Ferrite formation mechanism. In *Reactivity of Solids*, ed. J. Wood, O. Lindquist, C. Helgesson and N. G. Vannerberg. Plenum Press, New York, 1977, pp. 433–437.
6. Stuijts, A. L., Control of microstructures in ferrites. In *Ferrites: Proceedings of the International Conference*, ed. Y. Hoshino, S. Iida and M. Sugimoto. University of Tokyo Press, Tokyo, Japan, 1971, pp. 108–112.